Pharm Res (2011) 28:2820–2832
DOI 10.1007/s11095-011-0552-0

RESEARCH PAPER

New Fluorescent Probes Targeting the Mitochondrial-Located Translocator Protein 18 kDa (TSPO) as Activated Microglia Imaging Agents

Nunzio Denora • Valentino Laquintana • Adriana Trapani • Hiromi Suzuki • Makoto Sawada • Giuseppe Trapani

Received: 18 February 2011 / Accepted: 28 July 2011 / Published online: 5 August 2011

ABSTRACT

Purpose To evaluate the utility of new Translocator protein 18 kDa (TSPO)-targeted fluorescent probes for *in vivo* molecular imaging of activated microglia.

Methods Compounds 2–4 were synthesized; their stability and affinity for TSPO were determined. Compounds 2–4 were incubated both with Ra2 cells in the presence of LPS, a potent activator of microglia, and with tissue sections of normal and chemically injured brains. Compounds 2–4 were injected into carotid artery or directly in striatum of mice. Cells and tissue sections from these *in vitro* and *in vivo* studies were observed by fluorescence microscopy after histochemical treatments.

Results Compounds 2–4 are stable in both buffer and physiological medium and showed high affinity for TSPO and were found to stain live Ra2 microglial cells effectively. Double staining with Mito Tracker Red suggested that binding sites of compounds 2 and 3 may exist on mitochondria. *In vivo* studies showed that compounds 2–4 may penetrate in part into brain; moreover, cells in mouse striatum were stained with compounds 2–4 and microglial marker CD11b.

Conclusion Compounds 2–4 can fluorescently label activated microglia *in vitro* and *in vivo*.

N. Denora • V. Laquintana • A. Trapani • G. Trapani (✉)
Dipartimento Farmaco-Chimico, Facoltà di Farmacia
Università degli Studi di Bari
Via Orabona 4
70125 Bari, Italy
e-mail: trapani@farmchim.uniba.it

H. Suzuki • M. Sawada
Department of Brain Function,
Research Institute of Environmental Medicine, Nagoya University
Nagoya 464-8601, Japan

KEY WORDS activated microglia imaging · fluorescence microscopy. · imidazopyridine-compounds · TSPO

ABBREVIATIONS

FITC	fluorescein isothiocyanate isomer I
LPS	lipopolysaccharide
PBR	peripheral benzodiazepine receptor
PET	positron emission tomography
RBITC	rhodamine B isothiocyanate
TSPO	translocator protein 18 kDa

INTRODUCTION

Microglia cells are the largest population of macrophages in the brain and are thought to play a significant role in neurodegenerative disorders, such as Alzheimer's and Parkinson's disease, multiple sclerosis, and HIV-associated dementia (1). Microglia, indeed, undergo changes from a resting phenotype to an activated phenotype in response to a wide variety of Central Nervous System (CNS) imbalances. Measuring this microglia activation *in vivo* in patients suffering from such disorders can help to selectively monitor the progression of neuroinflammation as well as to assess efficacy of therapeutic protocols (2). Recent studies suggest that activated microglia in the CNS may be detected *in vivo* using positron emission tomography (PET) employing pharmacological ligands of the mitochondrial peripheral benzodiazepine receptor (PBR), which has recently been renamed as the Translocator protein 18 kDa (TSPO 18 kDa, TSPO) (3–5). TSPO is located at the contact sites between the outer and inner mitochondrial membranes and is associated with the mitochondrial permeability transition pore, where it regulates cholesterol transport and synthesis

of steroid hormones (6). However, TSPO has been implicated in other complex cellular functions, such as mediating apoptotic cell death (7), and, importantly, transition of microglia from the normal resting state to the activated one is associated with increased expression of TSPO. Because the binding capacity of TSPO to PBR ligands is very low in resting microglia, increased binding of ligands to TSPO may be used as a marker for detecting activated microglia *in vivo*. Thus, TSPO has become an attractive target not only for cancer imaging being overexpressed in a variety of cancers, but also as a marker of neuroinflammation (8), while the TSPO ligands can serve as biomarkers for diagnosis of neurodegenerative disorders (9).

Several TSPO-selective ligands have been developed, such as 2-phenylindole-3-acetamides (10), quinoline carboxamide (PK 11195) (11), benzodiazepines (Ro-54864) (12), Vinca alkaloids (e.g., vinpocetine) (5,13), phenoxyarylacetamides (DAA1106) (5,13), imidazo[1,2-a]pyridines (e.g., CLINME) (5,14), and pyrazolopyrimidines (e.g., DPA-713) (5,13). However, none of these TSPO ligands contains hydrophilic groups or organic functions such as amino-, hydroxy- and carboxylic-groups useful for further conjugation. Development of conjugable forms of TSPO ligands would allow their use as starting material for the formulation of diagnostic imaging agents.

In some of our early work, we showed that certain 2-phenyl-imidazo[1,2-*a*]pyridine acetamides are potent and selective ligands for TSPO, and they can be used as PET tracers for the translocator protein (15–17). More recently, we synthesized the first examples of conjugable imidazopyridinacetamides endowed with high affinity and selectivity for TSPO (18). Although a number of TSPO ligands labeled with ^{11}C and ^{18}F have been developed for activated microglia visualization by PET, their short half-life limits their use. A more practical approach to achieve this objective would be to conjugate the TSPO ligands with fluorescent probes. These efforts have been motivated by the fact that biological studies using radioisotopes are cumbersome and expensive in contrast to using fluorescence microscopy imaging. Therefore, the research and development of new fluorescent TSPO ligands for microglia visualization are actively pursued. Subsequent to the pioneering work on fluorescent TSPO ligands by Kozikowski *et al.* (19), several promising candidates, including the lanthanide chelate- and Lissamine-Rhodamine B dye-conjugate to a PK11195 analogue, (20–22), pyropheophorbides (23), and phenylindolglyoxylamides (24), have been proposed to potentially replace radioactive TSPO probes. In this context, it should be mentioned that the first example of TSPO-targeted nanocarrier delivering an imaging agent has been recently reported (25).

As part of our continued interest in developing new probes for the activated microglia visualization, we recently reported the synthesis and biological evaluation of 1 (Fig. 1) characterized by a 7-nitro-2,1,3-benzoxadiazol-4-yl fluorophore linked through a diamine spacer to 2-phenylimidazo [1,2-*a*]pyridine-3-acyl moiety (26). Compound 1 was shown to be an active derivative at micromolar level and represents a new fluorescent example for visualization of activated microglia and TSPO. It may have some significant advantages over the fluorescent or radioactive probes for TSPO currently used. However, in contrast to its calculated log C_{brain}/C_{blood} (log BB) value (27,28), compound 1 showed poor *in vivo* blood–brain barrier (BBB) penetration, presumably being a substrate for P-glycoprotein efflux protein (P-gp) or to extensive binding to serum proteins. Moreover, as observed for the majority of the fluorescent TSPO probes so far known, compound 1 is characterized by a moderate TSPO binding affinity at micromolar level.

In this paper, the design, syntheses and characterization of new fluorescent derivatives (i.e., the imidazopyridine compounds 2–4, Fig. 2) combining high affinity for TSPO, fluorescence emission at long wavelengths and favourable calculated log BB values (i.e., −0.78, −0.62, and −0.64 for compounds 2–4, respectively) are reported. The fluorescence features and *in vitro* and *in vivo* cell biology of these imidazopyridine compounds are reported and discussed.

MATERIALS AND METHODS

Melting points were determined in open capillary tubes with a Büchi apparatus and are uncorrected. IR spectra were obtained on a Perkin-Elmer IR Fourier Transform spectrophotometer in KBr pellets. Fluorescence and UV/VIS spectra were carried out, respectively, with a Perkin Elmer LS 55 luminescence Spectrometer and Perkin Elmer UV/VIS Lambda Bio20 Spectrometer. ^1H NMR spectra were determined on a Varian Mercury 300 MHz instrument. Chemical shifts are given in δ values referenced to

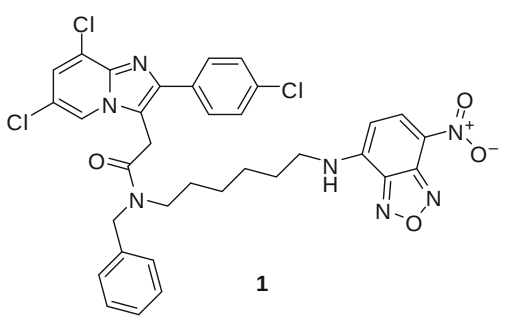

Fig. 1 Chemical structure of compound 1.

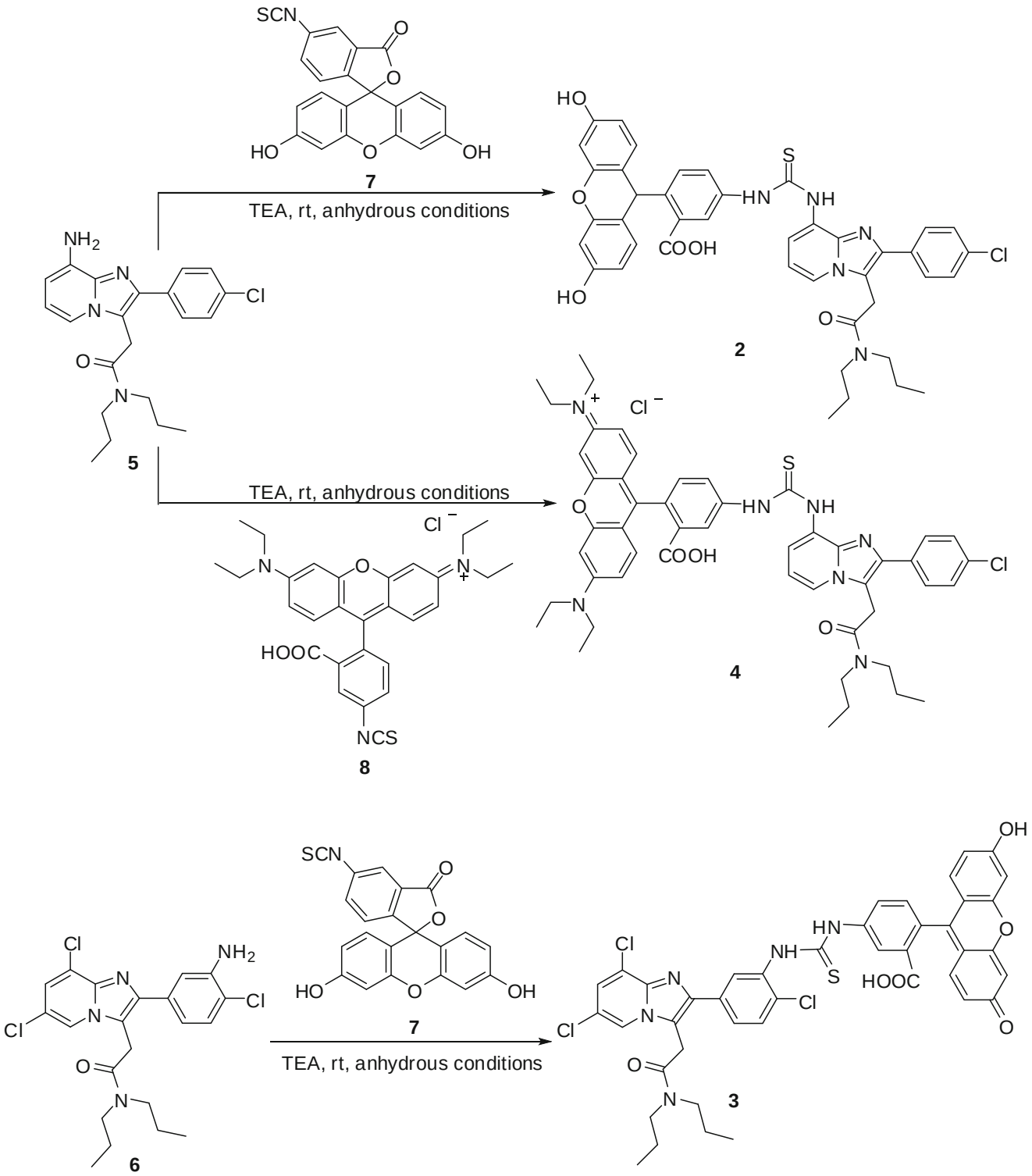

Fig. 2 Synthetic scheme for preparation of compounds 2–4.

the solvent. Mass spectra were obtained using an Agilent 1100 LC-MSD trap system VL instrument. Elemental analyses were carried out with a Eurovector (Milan, Italy) model EA 3000, and results were within ±0.40% of theoretical values. Silica gel 60 (Merck 70–230 or 230–400 mesh) was used for column chromatography. All the following reactions were performed under a nitrogen atmosphere and in dark conditions. The progress of the reactions was monitored by thin-layer chromatography (TLC) using Kieselgel 60F254 (Merck) plates.

The TSPO ligands *N,N*-di-*n*-propyl-[2-(8-amino-2-(4-chlorophenyl)imidazo[1,2-a]pyridin-3-yl)] acetamide (5) and *N,N*-di-*n*-propyl-[2-(2-(3-amino-4-chlorophenyl)-6,8-dichloroimidazo[1,2-a]pyridin-3-yl)] acetamide (6) were prepared according to synthetic procedures reported elsewhere (17). The starting triethylamine (TEA), fluorescein isothiocyanate isomer 1 (FITC) 7, rhodamine B isothiocyanate (RBITC) 8 anhydrous *N,N*-dimethylacetamide (DMF), and anhydrous tetrahydrofuran (THF) were purchased from Sigma-Aldrich (Italy). Commercial reagent grade chemicals and solvents were used without further purification. Fetal bovine serum (FBS) was purchased from EuroClone (Italy).

The synthesis of the TSPO-ligand-fluorescent conjugates 2–4 was accomplished as presented in Fig. 2. In particular, compounds 2 and 4 were obtained by reaction of the TSPO ligand *N,N*-di-*n*-propyl-[2-(8-amino-2-(4-chlorophenyl)imidazo[1,2-a]pyridin-3-yl)]acetamide (5) with the isothiocyanate fluorescent probes FITC 7 and RBTC 8, respectively, whereas conjugate 3 was prepared by reacting the PBR ligand *N,N*-di-*n*-propyl [2-(2-(3-amino-4-chlorophenyl)-6,8-dichloroimidazo[1,2-a]pyridin-3-yl)] acetamide (6) with isothiocyanate FITC 7 in the presence of TEA and under anhydrous conditions. All compounds were fully characterized by IR, ^{1}H NMR, mass spectra, and elemental analyses. The yields and physical data for the final compounds are reported in Table I.

General Procedure for Preparation of TSPO-Ligand Fluorescent Compounds 2–4

To a stirred and ice-cooled solution of the appropriate TSPO-ligand 5 or 6 (0.25 mmol) in anhydrous DMF (5 ml), TEA (0.3 mmol) was added. After 10 min, a solution of the suitable isothiocyanate fluorescent probe (0.20 mmol; 7 or 8) in anhydrous DMF (1 ml) was added drop-wise, and the stirring was prolonged for 1–2 h at room temperature in the dark. Solvent was evaporated under reduced pressure, and the residue was dissolved in CH_2Cl_2 (20 ml), washed twice with a 5% $NaHCO_3$ aqueous solution, and dried (Na_2SO_4). Next, the organic solvent was evaporated under reduced pressure, and the resulting residue was purified by silica gel column chromatography [$CHCl_3/CH_3OH$ 9/1 (v/v) as eluent] to give the desired product (2–4) as powder.

5-(3-(2-(4-chlorophenyl)-3-(2-(dipropylamino)-2-oxoethyl)imidazo[1,2-a]pyridin-8-yl)thioureido)-2-(3,6-dihydroxy-9H-xanthen-9-yl) benzoic acid (2): IR (KBr): 3418, 1757, 1615, cm^{-1}; ^{1}H NMR (DMSO-d_6) δ: 0.7–0.9 (m, 6H, CH_3), 1.4–1.8 (m, 4H, CH_2), 3.2–3.4 (m, 4H, CH_2N), 4.22 (s, 2H, CH_2CO), 6.4–6.7 (m, 7H, Ar), 6.8–7.1 (m, 1H, Ar), 7.23 (d, J=8.25 Hz, 1H, Ar), 7.51 (d, J=8.52 Hz, 2H, Ar), 7.67 (d, J=8.52 Hz, 2H, Ar), 7.8–8.1 (m, 3H, Ar), 10.0–11.1 (br, 2H, $(NH)_2CS$); MS (ESI) *m/z* 772.3 $[M-H]^-$; Anal. ($C_{42}H_{36}ClN_5O_6S$) C, H, N.

5-(3-(2-chloro-5-(6,8-dichloro-3-(2-(dipropylamino)-2-oxoethyl) imidazo[1,2-a]pyridin-2-yl)phenyl)thioureido)-2-(3,6-dihydroxy-9H-xanthen-9-yl)benzoic acid (3): IR (KBr): 3442, 1759, 1620, cm^{-1}; ^{1}H NMR (DMSO-d_6) δ: 0.77 (t, J=7.4 Hz, 3H, CH_3), 0.86 (t, J=7.4 Hz, 3H, CH_3),1.4–1.7 (m, 4H, CH_2), 3.2–3.4 (m, 4H, CH_2N), 4.32 (s, 2H, CH_2CO), 6.5–6.7 (m, 6H, Ar), 7.1–7.3 (m, 2H, Ar), 7.5–7.9 (m, 4H, Ar), 8.2–8.6 (m, 2H, Ar), 9.8–10.2 (br, 2H, $(NH)_2CS$); MS (ESI) *m/z* 840.0 $[M-H]^-$; Anal. ($C_{42}H_{34}Cl_3N_5O_6S$) C, H, N.

N-(9-(2-carboxy-4-(3-(2-(4-chlorophenyl)-3-(2-(dipropylamino)-2-oxoethyl)imidazo[1,2-a]pyridin-8-yl)thioureido)phenyl)-6-(diethylamino)-3H-xanthen-3-ylidene)-N-ethylethanaminium chloride (4): IR (KBr): 3435, 1733, 1645 cm^{-1}; ^{1}H NMR ($CDCl_3$) δ: 0.77 (t, J=7.4 Hz, 3H, CH_3), 0.85 (t, J=7.4 Hz, 3H, CH_3), 1.25 (t, J=7.4 Hz, 12H, CH_3), 1.3–1.7 (m, 4H, CH_2), 3.1–3.5 (m, 12H, $CH_2NCO+CH_2N$), 4.07 (s, 2H, CH_2CO), 6.1–7.2 (m, 8H, Ar), 7.32 (d, J=8.25 Hz, 2H, Ar), 7.3–7.5 (m, 1H, Ar), 7.54 (d, J=8.25 Hz, 2H, Ar), 7.7–8.1 (m, 2H, Ar), 8.19 (s, 1H, Ar), 9.0–10.0 (br, 2H, $(NH)_2CS$); MS (ESI) *m/z* 882.1 $[M-H]^-$; Anal. ($C_{50}H_{55}ClN_7O_4S$) C, H, N.

Stability Studies on Compounds 2–4

The chemical and physiological stabilities of compounds 2–4 were determined in 0.05 M phosphate buffer pH 7.4 and in diluted (50% v/v) FBS solution at 37°C, respectively. All experiments were done in triplicate; half-lives, reported in Table I, were measured by the disappearance of the tested compound.

Table I Yields, Affinity for Rat Cerebrocortical TSPO 18 kDa, Maximum Excitation and Emission Wavelengths and Chemical and Enzymatic Stability of Compounds 2–4

Compound	Yield (%)	TSPO 18 kDa IC_{50} (nM)	λ_{max}Ex nm	λ_{max}Em nm	$t_{1/2}$ (h) Phosphate Buffer 0.05 M (pH 7.4)	$t_{1/2}$ (h) diluted FBS
1	55	6700	465	541	–	–
2	42	8.34	499	520	131 ± 3	>24
3	38	0.95	493	516	70 ± 2	>24
4	23	12.83	545	568	128 ± 4	>24

Chemical Stability

Stability studies were carried out at controlled temperature (37±0.2°C) in a water bath in dark condition. The chemical stability of compounds 2–4 was studied in isotonic 0.05 M phosphate buffer at pH 7.4. The experiments were carried out by adding a stock solution of the test compounds in CH_3OH (~ 1.0 mg/ml) to 1 ml of the buffer solution preheated at 37°C. The final concentration of the resulting solutions was 100 μM. The test solutions were vortexed and maintained in a shaker water bath at a constant temperature of 37±0.2°C. At appropriate time intervals, 20 μl aliquots were removed and immediately analyzed by high performance liquid chromatography (HPLC). Pseudo-first-order rate constants for the hydrolysis of the derivatives were determined from the slopes of linear plots of the logarithms of residual compound against time. HPLC analyses were performed with a Waters Associates model 600 pump equipped with a Waters 990 variable wavelength UV detector and a 20 μl loop injection valve. A reversed phase Waters Bondapak C18 (15–20 μm particles, 19×300 mm) column was used in conjunction with a SecurityGuard Phenomenex pre-column. Analytes were eluted with mixtures of methanol/10 mM phosphate buffer pH 60:40 (v/v). The injected volume was 20 μl. The flow rate of 0.8 ml/min was maintained, and the column effluent was monitored continuously at 254 nm. The compounds were estimated by measuring the peak areas or peak heights in relation to those of standards chromatographed under identical conditions.

Stability in Physiological Medium

The stability of compounds 2–4 in physiological medium was studied at 37±0.2°C in 0.05 M phosphate-buffered saline (0.14 M NaCl) at pH 7.4 containing 50% v/v of FBS. The final concentration of the test compounds in the physiological medium was 100 μM. The resulting test solution was maintained at 37±0.2°C in a shaking water bath. Aliquots of 50 μl were withdrawn at appropriate time intervals and diluted with 200 μl of cold acetonitrile to precipitate the serum proteins. After mixing and centrifugation for 5 min at 13200 rpm, the supernatant was first filtered and then analyzed by HPLC as described previously.

Receptor Binding Assays

Adult male or female Sprague–Dawley CD rats (Charles River, Como, Italy) with body masses of 200–250 g at the beginning of the experiments were maintained under an artificial 12-h light/dark cycle (light on from 8:00 a.m. to 8:00 p.m.) at a constant temperature of 23 (2°C and 65% humidity. Food and water were freely available, and the animals were acclimated for >7 days before use. Experiments were performed between 8:00 a.m. and 2:00 p.m. Animal care and handling throughout the experimental procedure were performed in accordance with the European Communities Council Directive of 24 November 1986 (86/609/EEC). The experimental protocols were approved by the Animal Ethical Committee of the University of Cagliari. After sacrifice, the brain was rapidly removed, the cerebral cortex was dissected, and tissues were stored at −80°C until assay.

[^{3}H]PK11195 Binding

The tissues were thawed and homogenized in 50 volumes of Dulbecco's phosphate-buffered saline (PBS; pH 7.4) at 4°C with a Polytron PT 10 (setting 5, for 20s). The homogenate was centrifuged at 40000*g* for 30 min, and the pellet was resuspended in 50 volumes of PBS and recentrifuged. The new pellet was resuspended in 20 volumes of PBS and used for the assay. [^{3}H]PK11195 binding was determined in a final volume of 1,000 μl of tissue homogenate (0.15–0.20 mg of protein), 100 μl of [^{3}H]PK11195 (specific activity 85.5 Ci/mmol, New England Nuclear) at a final assay concentration of 1 nM, 5 μl of drug solution or solvent, and 795 μl of PBS buffer (pH 7.4 at 25°C). Incubations (25°C) were initiated by the addition of membranes and were terminated 90 min later by rapid filtration through glass-fiber filter strips (Wathman® GF/B), which were rinsed five times with 4 ml of ice-cold PBS buffer using a Cell Harvester filtration manifold (Brandel). Filter-bound radioactivity was quantified by liquid scintillation spectrometry. Non-specific binding was defined as binding in the presence of 10 μM unlabeled PK11195 (Sigma-Aldrich, St. Louis, MO).

In Vitro Studies on Compounds 2–4

Cell Culture

Ra2, an immortalized microglial clone, was established from a mouse primary microglial culture and maintained in Eagle's minimum essential medium (MEM) supplemented with 10% calf serum, 5 μg/ml bovine insulin, 0.2% glucose, and 1 ng/ml recombinant mouse granulocyte-macrophage colony stimulating factor (Genzyme, Cambridge, MA), which is essential for Ra2 growth in culture.

Ra2 cells were seeded at a density of 6,500 cells per cm^2 on a glass of a glass-bottom dish (Matsunami Glass IND. Ltd., Osaka, Japan), then cultured for 24 h. Ra2 cells were incubated with compounds 2, 3, and 4 at a final concentration of 0.1 μM for 2 h, followed by the addition of Mito Tracker red after 15 min (a dye useful for staining mitochondria in live cells) (Molecular Probe, Eugene, OR)

with incubation at 37°C for 1 h. After the treatment, Ra2 cells were observed by a fluorescent microscope and photographed. Then the cells were incubated for 24 h with 1 μg/ml lipopolysaccharide (LPS) (Sigma-Aldrich, St. Louis, MO), which is an endotoxin from *E. coli* and a potent activator of microglia. The effect of microglial activation was observed by a fluorescent microscope and photographed.

Tissue Sections

Frozen tissue sections (10 μm thickness) of normal and chemically injured brains from male Wistar rats were cut in a cryostat and mounted on slides and dried. Then sections were fixed by 4% paraformaldehyde at room temperature for 15 min. After washing with phosphate-buffered solution (pH 7.2) twice, sections were incubated with 0.1 nM of compound 2–4 and fluorescent dye labeled with either isolectin B4 (TRITC-conjugates, Cat # L9831 for compound 2 and 3, or FITC-conjugates, Cat # L2895 for compound 4, Sigma, St. Louis, MO) at 4°C for 16 h, washed with PBS twice, then incubated with 4',6-diamidino-2-phenylindole (DAPI) at room temperature for 30 min. Sections were observed by a fluorescent microscope and photographed.

In Vivo Studies on Compounds 2–4

Arterial Injection

Adult male C57BL/6 mice were deeply anesthetized with sodium pentobarbital (25 mg/kg, i.p.) before surgery and remained under anaesthesia throughout the procedure. When spinal reflexes were absent, a transverse incision was made to expose the right carotid artery. After the temporary occlusion of proximal site of the carotid artery with aneurysm clip, a small pole was made in the distal site of the artery with a 27-gauge needle, and a polyethylene tube (Becton Dickinson, USA) was inserted into the proximal site of the artery from the pole. After the aneurysm clip was released, 0.2 ml of one of the compound solutions (10 μM in the final concentration) or the same volume of Fluorescein isothiocyanate-labeled dextran (FITC-dextran) (Sigma, St. Louis, MO, average molecular weight over 250,000; 5 μM in the final concentration) were injected as a bolus over 30 s into the carotid artery via the polyethylene tube. The injected drug test solution was obtained from a stock solution (2.9 mM) in dimethylsulfoxide, which was in turn diluted to 10 μM with PBS. At 24 h post injection, animals were additionally anesthetized, and their blood was washed out by trans-cardial perfusion of an excess amount of isotonic saline solution. Then brains, lungs, and livers were removed, frozen in liquid nitrogen, and embedded in OTC compound (Tissue Tek, Elkhart, IN). Coronal sections (8 μm) were cut in a cryostat and mounted on slides and dried. Then sections were fixed by 4% paraformaldehyde. Fluorescent observation was performed with a fluorescence microscope (OLYMPUS BX50, Japan).

Intracranial Injection

Adult male C57BL/6 mice were deeply anesthetized with sodium pentobarbital (25 mg/kg, i.p.) as mentioned above. A sagittal incision (1.5 cm) was made with a sterile scalpel (#15 blade). A small (1.2 mm diameter) hole was opened with a sterilized drill bit at coordinates anterior-posterior (AP +0.5 mm) and lateral (L −2.0 mm, left), using intermittent action to prevent heat injury to the area. The sterilized 5 μl Hamilton syringe (26 s gauge; 0.47 mm outer diameter) loaded with 10 μM of compound solution (or FITC-dextran for the control) was vertically aligned in the stereotaxic apparatus, then inserted into the opened hole at the coordinates of the striatum (AP: +0.5; L: −2.0 and DV: −3.0 mm, below pial surface7). The solution was injected at a flow rate of 0.1 μl/min. At 24 h after injection, animals were additionally anesthetized and perfused with isotonic saline. Brain sections were prepared as mentioned above. All procedures of animal experiments were conducted in accordance with the Guidelines for Nagoya University Animal Experimentation.

Immunohistochemical Staining

Frozen sections (10 μm) of the brains were cut with a cryostat microtome, transferred to a MAS-coated slide glass (Matsunami Glass IND., Ltd., Osaka, Japan) and immediately air-dried. The sections were fixed with 4% paraformaldehyde in PBS for 10 min at room temperature, incubated in a blocking buffer for 30 min at room temperature, labeled with antibodies against CD11b (BMA Biomedicals, Augst, Switzerland) at a dilution of 1:100 for 2 h at 37°C, then reacted with HRP-conjugated goat anti-mouse IgG (Nichirei Bioscience, Tokyo, Japan) at a dilution of 1:200 for 30 min at room temperature. They were visualized with DAB staining kit (Nichirei Bioscience, Tokyo, Japan) and counterstained with HE staining solution for 5 min at room temperature. Photographs of sections were taken under a fluorescent microscope BX50 (Olympus, Japan) equipped with a CCD camera Cool Snap HQ (Photometrics, AZ, USA).

Densitometric Analysis

Some of the digital photographs were quantitatively analyzed by ImageJ 1.44 software (Research Services Branch, National Institute of Mental Health, Bethesda, Maryland, USA). Quantitative values of cytosolic fluorescence in Ra2 microglia were determined as average values of ten cytosolic areas sampled randomly.

RESULTS

All the TSPO fluorescent ligands 2–4 were found to be very stable in both buffer and physiological medium with half-lives >24 h (see Table I). Compounds 2–4 showed a visible fluorescence, and the optimum excitation and emission wavelengths are summarized in Table I. The data were recorded in methanol as solvent using a Kontron UV–vis spectrometer and a Perkin-Elmer LS-50B spectrofluorometer. As can be seen from Table I, compounds 2–4

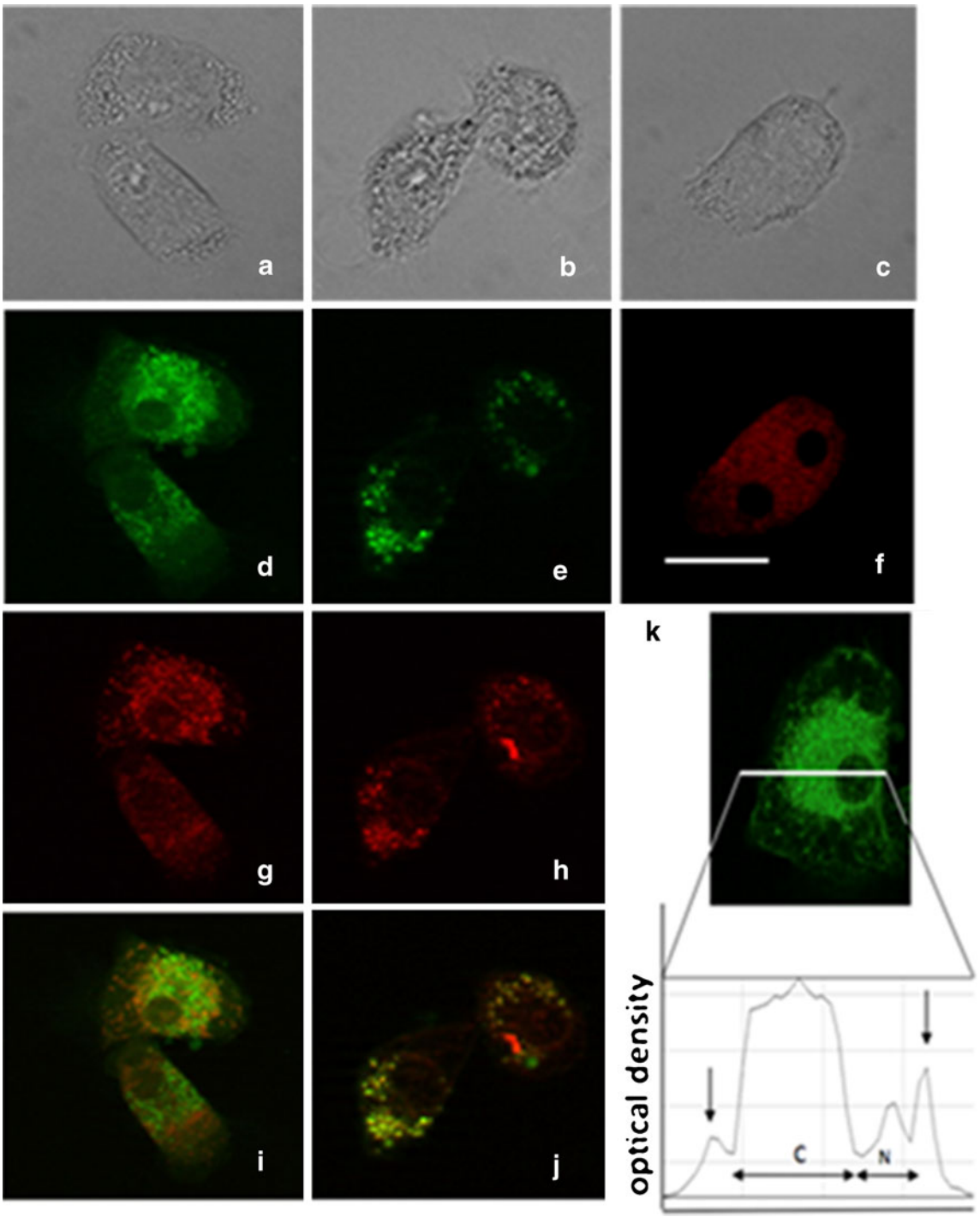

Fig. 3 Fluorescent images of Ra2 microglia stained with compounds 2, 3, 4. Ra2 cells were incubated with compound 2 (**a, d, g, i**), 3 (**b, e, h, j**) and 4 (**c, f**) at a final concentration of 0.1 μM for 2 h followed by the addition of Mito Tracker red after 15 min. (**a, b, c**) Phase contrast images; (**d,e, f**) fluorescent images; (**g, h**) fluorescent images of Mito Tracker Red; (**i, j**) overlay images of compound fluorescence and Mito Tracker Red; (**k**) quantitative analysis of fluorescence distribution of compound 2 in a Ra2 cell. Scale bar: 20 μm.

exhibited fluorescence emission maxima in the range of 516–568 nm, implying their usefulness in visual imaging of TSPO.

Radioligand Binding Assays

The affinity of compounds 2–4 for TSPO was assessed by measuring their ability to displace [^{3}H]PK11195 from binding to membrane preparations of cerebral cortex. Their effects were compared with those of unlabeled PK11195, and the results of these analyses are shown in Table I. As can be seen, compounds 2–4 showed high affinity for TSPO.

In Vitro Studies on Compounds 2–4

Compounds 2–4 were found to stain live Ra2 microglia cells effectively (Fig. 3). Intense fluorescence more than 20 times higher than background fluorescence was observed as a deposit-like pattern mainly distributed in cytosol (Fig. 3k).

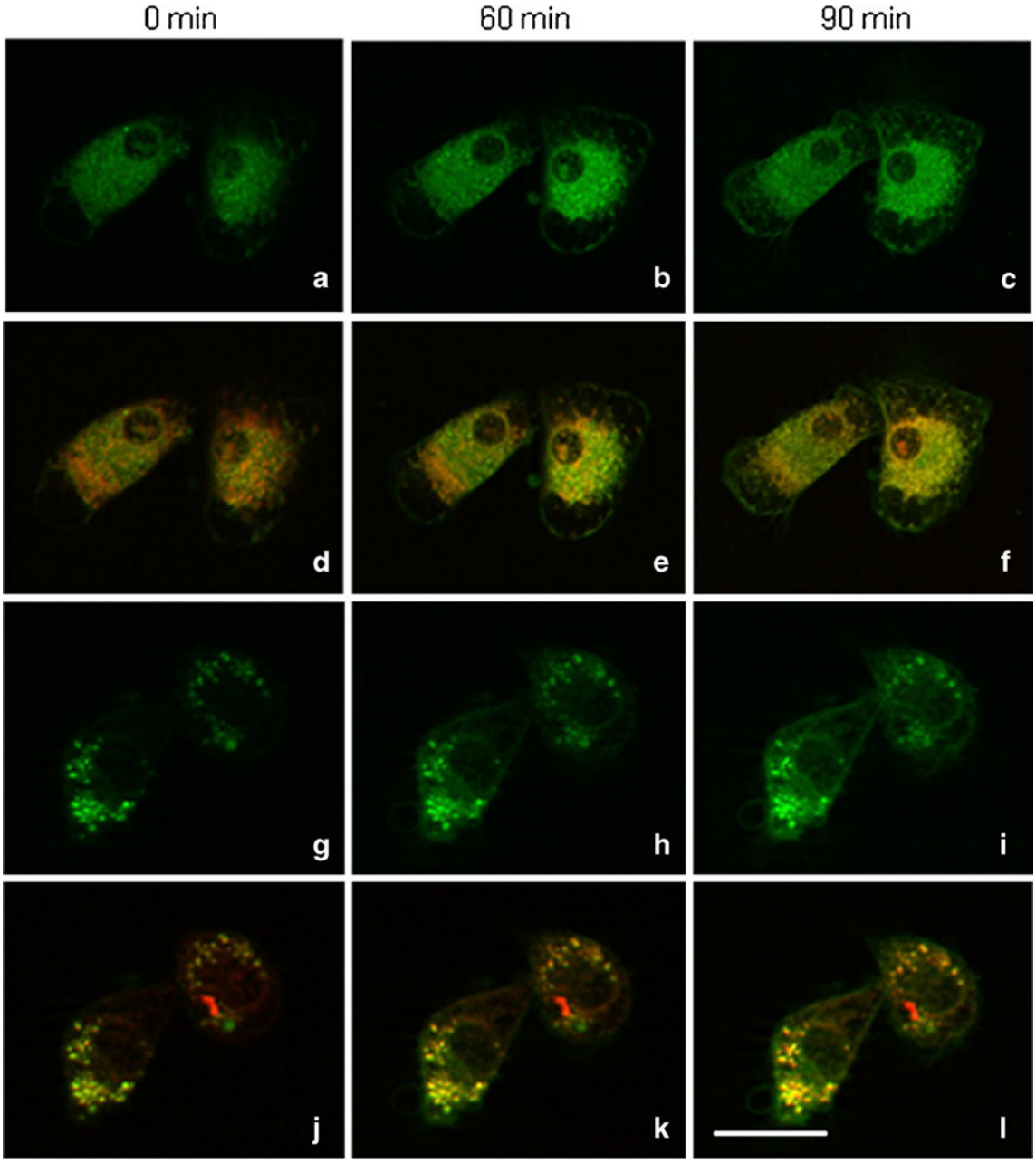

Fig. 4 Changes of fluorescent intensity of compounds 2 and 3 in Ra2 cells during microglial activation. Ra2 cells stained with compounds 2 (**a–f**) or 3 (**g–l**) were incubated with 1 μg/ml lipopolysaccharide for 0 (**a, d, g, l**), 60 min (**b, e, h, k**) and 90 min (**c, f, i, l**). (**a–c, g–i**) Fluorescent images of compound 2 (**a–c**) and 3 (**g–h**). (**d–f, j–l**) Fluorescent images of each compound and Mito Tracker Red. Scale bar: 20 μm.

Plasma membrane was also positive in fluorescence at intensity of a one half to one third of cytosol (Fig. 3k). Very low or no staining of nucleus and vacuoles were observed. Many fluorescence-positive deposits in compounds 2 and 3 were stained with Mito Tracker Red (Fig. 3). Non-specific large deposits were not observed, which were not stained with Mito Tracker Red. The intensity of fluorescence was increased by microglial activation with LPS (Fig. 4); in a typical measurement of the change of intensity, average of optical density values of cytosol was 69.7 ± 8.3 before LPS stimulation, 150.6 ± 15.3 at 60 min and 132.8 ± 14.7 at 90 min after LPS stimulation.

In the brain sections, compounds 2 and 3 stained brain cells in a non-specific manner; however, they were found to stain activated microglia in injured brain area effectively (Fig. 5A, B, a, b, c: compound 2; Fig. C, D, d, e, f: compound 3). Compound 4 indicated high background fluorescence; the S/N ratio of cerebral cortex area of brain section stained by compound 4 was less than 2.3. The fluorescent cells in the injured brain sections were labeled with isolectin B4 (Fig. 6), a marker for activated microglia.

In Vivo Studies on Compounds 2–4

After injection in carotid artery of adult male C57BL/6 mice of compounds 2, 3, 4 or FITC-dextran, used as a control dye, and successive brain removal, it was found that the distribution of staining with the compounds indicated was observed in brain parenchymal cells and blood vessels (Fig. 7); this pattern was different from that of FITC-dextran, which hardly penetrated into brain because of existence of the BBB. These results indicate that certain parts of compound 2–4 may penetrate into brain and other parts may remain in endothelial cells of blood vessels.

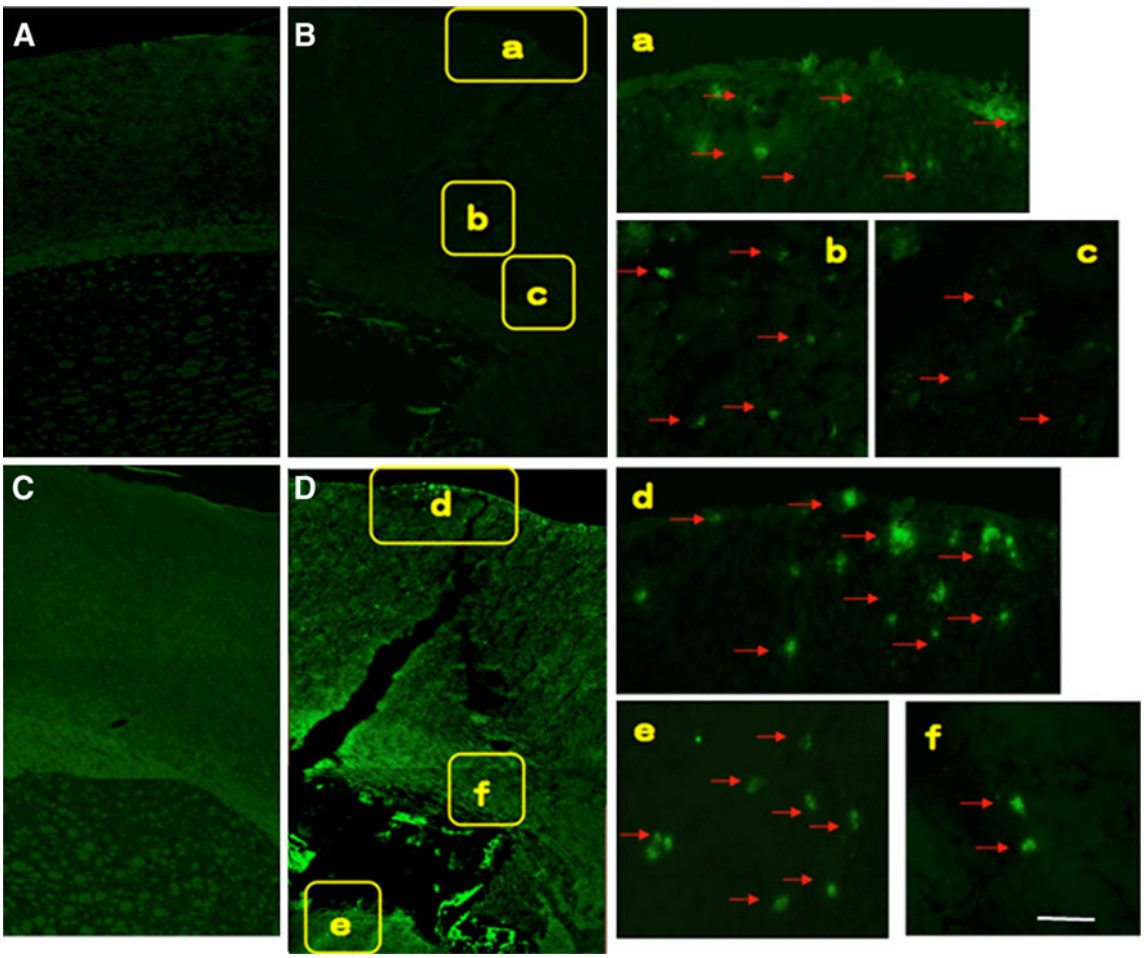

Fig. 5 Compounds 2 and 3 reacted with brain cells in injured brain sections. Brain sections from normal (**A**, **C**) or chemically injured rats (**B**, **D**) were incubated with 0.1 nM of compounds 2 (**A**, **B**, **a**, **b**, **c**) and 3 (**C**, **D**, **d**, **e**, **f**). (**a**–**f**) Higher magnification optics. Arrows: indicate fluorescent-positive cells in brain sections. Scale bar: 50 μm.

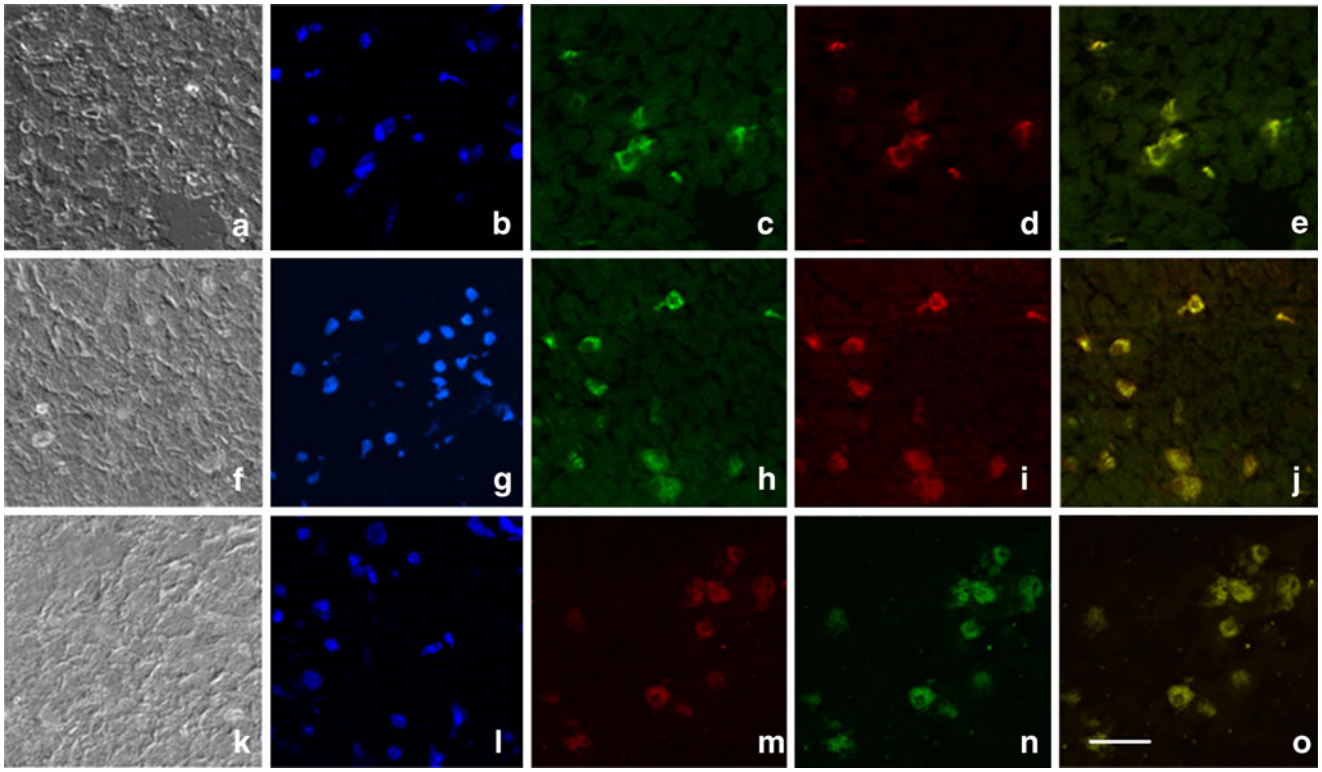

Fig. 6 Compounds 2, 3 and 4 reacted with microglia in injured brain sections. Brain sections from chemically injured rats were incubated with 0.1 nM of compounds 2 (**a–e**), 3 (**f–j**) and 4 (**k–o**) then stained with and fluorescent dye-labeled isolectin B4. (**a, f, k**) phase optics; (**b, g, l**) DAPI fluorescent images; (**c, h, m**) fluorescent images of compounds 2 (**c**), 3 (**h**) and 4 (**m**); (**d, i, n**) fluorescent images of isolectin B4 staining; (**e, j, o**) overlay images of each compound and isolectin B4 staining. Scale bar: 50 μm.

In order to eliminate the effect of blood vessels for identification of the target of the compounds in the brain of live animals, compounds 2–4 were injected into mouse striatum directly. Cells in the mouse striatum were stained with compounds 2–4, which were also labeled with CD11b antibody (Fig. 8), a microglial marker.

DISCUSSION

The aim of this work was to develop new fluorescent probes targeting the TSPO as activated microglia imaging agents. TSPO is primarily expressed on the mitochondria, and it is over-expressed in a variety of different pathological states, including neuroinflammation, where activated microglia occurs. For the mentioned purpose, imidazopyridine compounds 2–4 were designed to possess high affinity and selectivity for TSPO on the basis of the structure-affinity relationships previously developed by us in this series of TSPO ligands (16). Indeed, receptor binding studies confirmed that compounds 2–4 possess a 1,000-fold improved receptor affinity (nanomolar level) in comparison to that of 1. Within the series, compound 3 showed the highest affinity (e.g., 0.95 nM, about 9- and 12-fold more active than 2 and 4, respectively), indicating that introduction of the fluorescein moiety on the phenyl group of the 2-phenylimidazopyridine nucleus leads to a more favourable interaction with the receptor. On the other hand, comparing the affinities of the imidazopyridines 2 and 4 bearing the fluorescent probe at 8-position suggest that introducing rhodamine B moiety negatively affects binding affinity. In terms of binding affinity, the fluorescent probes for TSPO in series 2–4, to the best of our knowledge, are one of the most active compounds. In fact, the probe recently described by Taliani *et al.* (24), although characterized by a TSPO binding affinity at nanomolar level (i.e., 42.2 nM), is less active than 2–4 (i.e., 8.34, 0.95 and 12.83 nM, respectively).

The results of cell biology and fluorescence microscopy studies suggest that the binding sites of compounds 2 and 3 may exist on mitochondria (Fig. 3), as confirmed by the fact that many fluorescence-positive deposits in compounds 2 and 3 were stained with Mito Tracker Red. Moreover, since the fluorescent cells in the injured brain sections were labeled with isolectin B4 (Fig. 6), compounds 2–4 may have the potential to react with activated microglia in the brain.

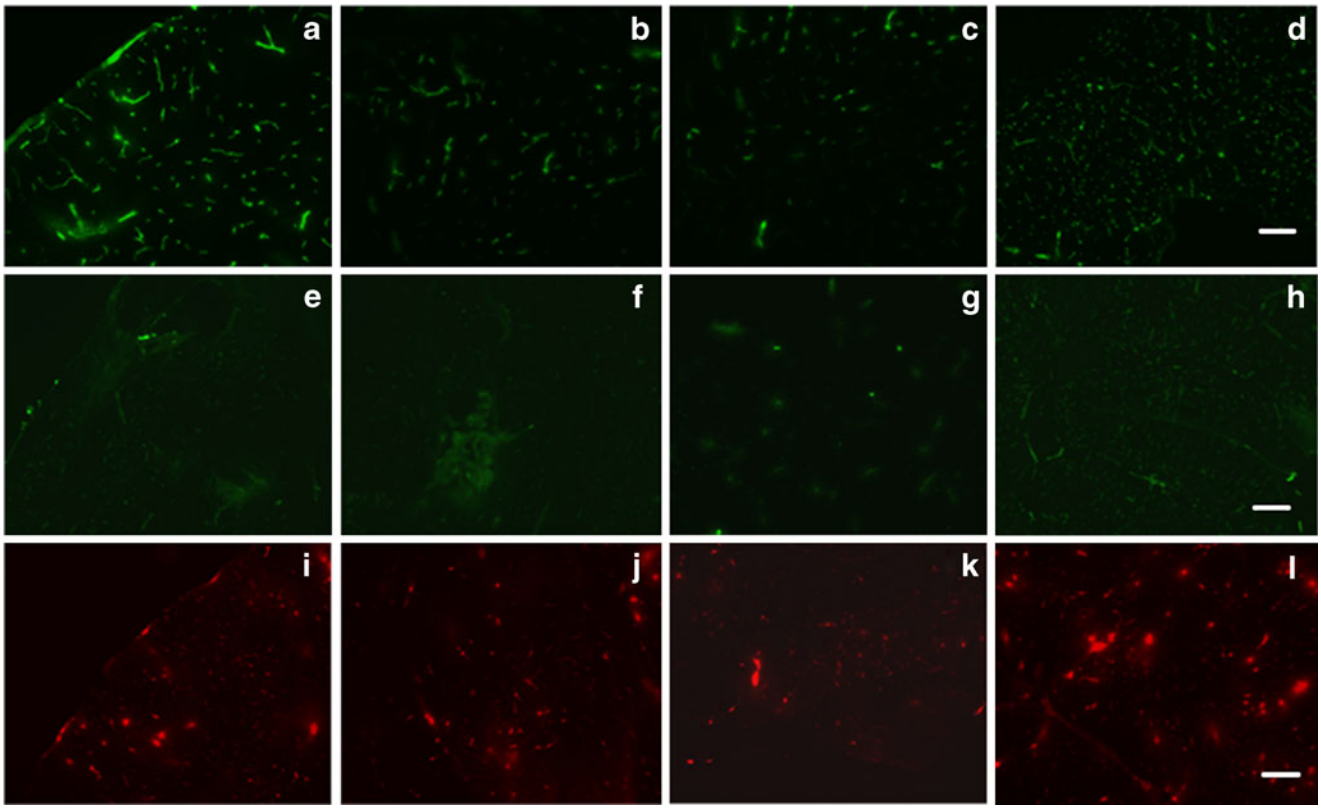

Fig. 7 *In vivo* distribution of compounds 2, 3 and 4. One of compound 2 (**a–d**), 3 (**e–h**) and 4 (**i–l**) was injected into mouse carotid artery, then brain sections were prepared. (**a, e, i**) Cerebral cortex; (**b, f, j**) hippocampus; (**c, g, k**) hypothalamus; (**d, h, l**) brainstem. Scale bar: 50 μm.

Finally, results from intracranial injection of 2–4 study clearly indicate that they can label microglia effectively even in live animals. These results demonstrate that the fluorescein derivatives 2 and 3 are more effective than the rhodamine B analogue 4 in labeling microglia. Interestingly, this trend parallels with the binding affinity rank order observed.

A comparison of compounds 2–4 with our former fluorescent ligand 1 reveals that while ligand 1 was observed to associate with plasma membrane (26), compounds 2–4 showed intense fluorescence as a deposit-like pattern mainly distributed in cytosol, and faint fluorescence was observed to localize in plasma membrane (Fig. 3k), suggesting that enhancement of the binding affinity in the imidazopyridine series of TSPO ligands may be favourable to visualize mitochondria in cytosol and to effectively label activated microglia. Moreover, it is interesting to compare the BBB penetration properties of 1 with those of 2–4 on the basis of the log BB value as estimated by the Clark's model (27). This model relates log BB to log P and polar surface area, a descriptor computed with a fragment-based approach known as the topological PSA (TPSA) approach (28). It is generally accepted that compounds with log BB >0.3 cross the BBB readily, whereas compounds with log BB<−1.0 are poorly distributed to the brain. On the basis of the predicted log BB values, compound **1** should be able to cross the BBB better than 2–4 (i.e., log BB −0.54 of 1 compared with −0.78, −0.62, and −0.64 for compounds 2–4, respectively, using an online available software for log P and TPSA calculation (http://www.molinspiration.com)). Indeed, our experimental data indicate that compounds 2–4 possess good BBB penetration properties *in vivo*. Probably, the pharmacokinetic limitations to account for the poor BBB penetration of 1 (i.e., the possibility that this compound is a substrate of P-gp or that it is extensively bound to serum proteins) does not occur for 2–4, which makes them valuable agents for activated microglia visualization.

Compounds 2–4 may have some significant advantages over other currently known fluorescent probes for TSPO. Thus, a comparison with the indoleacetamide reported by Kozikowski *et al.* (19) with the Lissamine-Rhodamine B dye-PK11195 analogue conjugate (21) and the fluorescent probe described by Taliani *et al.* (24), all characterized by simple structure, reveals that compounds 2–4 should possess better BBB penetration properties on the basis of their log BB values (i.e., −0.78, −0.62, and −0.64 for compounds 2–4, compared with −1.06 of indoleacetamide, −1.78 of the

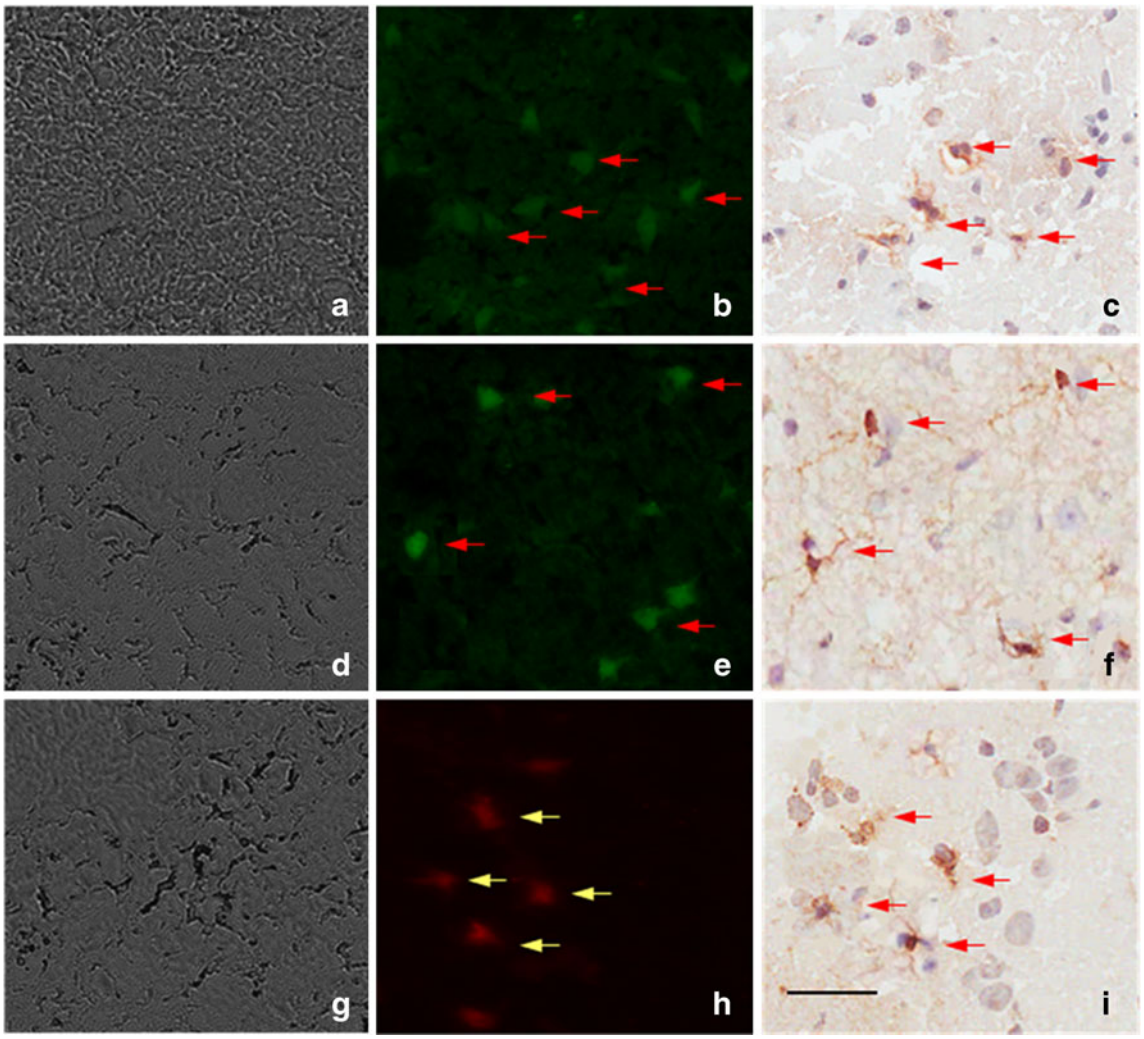

Fig. 8 Intracranial injection indicates the compounds have reacted with CD11b-positive microglia. One of compound 2 (**a–c**), 3 (**d–f**) and 4 (**g–i**) was injected into mouse striatum. Brain sections were stained with anti-CD11b antibody. (**a, d, g**) Phase contrast images; (**b, e, h**) fluorescent images; (**c, f, i**) CD11b staining. Arrows: double positive cells in brain sections. Scale bar: 50 μm.

PK11195 analogue and −1.39 of Taliani *et al.* probe, as estimated by Clark's model (27)).

CONCLUSION

In this work, cell biology and fluorescence microscopy studies reveal that the new fluorescent probes 2–4 should possess good BBB penetration properties and are able to label activated microglia *in vitro* and *in vivo*. In particular, the imidazopyridines 2 and 3, bearing the fluorescein moiety, are the most active derivatives. They may have some significant advantages (structural simplicity, cost-effective, easy to handle) not only over the previously studied compound 1 but also over most currently used fluorescent probes for TSPO. Therefore, compounds 2–4, especially 2 and 3, may be new useful tools of bio-imaging for TSPO alternative to PET. Such compounds with high affinity to the mitochondrial protein TSPO may be valuable tools for the diagnosis of neuroinflammation and neurodegenerative disorders.

ACKNOWLEDGMENTS & DISCLOSURES

This work was supported by grants from Ministero dell'Universita` e della Ricerca Scientifica e Tecnologica (MIUR) (COFIN 2006 of G.T.) and from Università degli Studi di Bari (Iniziative d'Ateneo 2006). We thank Prof. Giovanni Biggio (University of Cagliari, Italy), Mr. Giovanni Dipinto (University of Bari), and Mr. Antonio Palermo (University of Bari) for help in receptor binding studies and

skilful technical assistance in recording mass spectra and ^{1}H-NMR spectra, respectively. The authors are very grateful to Dr. Sandeep Dhareshwar (Novartis) for his revision of this manuscript.

REFERENCES

1. Venneti S, Lopresti BJ, Wiley CA. The peripheral benzodiazepine receptor (Translocator protein 18 kDa) in microglia: From pathology to imaging. Progr Neurobiol. 2006;80:308–22.
2. Cagnin A, Brooks DJ, Kennedy AM, Gunn RN, Myers R, Turkheimer FE. In-vivo measurement of activated microglia in dementia. Lancet. 2001;358:461–7.
3. Papadopoulos V, Baraldi M, Guilarte TR, Knudsen TB, Lacapere JJ, Lindemann P, *et al.* Translocator protein (18 kDa): new nomenclature for the peripheral-type benzodiazepine receptor based on its structure and molecular function. Trends Pharmacol Sci. 2006;27:402–9.
4. Cicchetti F, Brownell AL, Williams K, Chen YI, Livni E, Isacson O. Neuroinflammation of the nigrostriatal pathway during progressive 6-OHDA dopamine degeneration in rats monitored by immunohistochemistry and PET imaging. Eur J Nerurosci. 2002;15:991–8.
5. Schweitzer PJ, Fallon BA, Mann JJ, Kumar JS. PET tracers for the peripheral benzodiazepine receptor and uses thereof. Drug Discov Today. 2010;15:933–42.
6. Papadopoulos V, Lecanu L, Brown RC, Han Z, Yao Z-X. Peripheral-type benzodiazepine receptor in neurosteroid biosynthesis, neuropathology and neurological disorders. Neuroscience. 2006;138:749–56.
7. Costantini P, Jacotot E, Decaudin D, Kroemer G. Mitochondrion as a novel target of anticancer chemotherapy. J Natl Canc Inst. 2000;92:1042–53.
8. Banati RB. Visualizing microglial activation in vivo. Glia. 2002;40:206–17.
9. Doorduin J, de Vries EFK, Dierckx RA, Klein HC. PET imaging of the peripheral benzodiazepine receptor: monitoring disease progression and therapy response in neurodegenerative disorders. Curr Pharmaceut Des. 2008;14:3297–315.
10. Romeo E, Auta J, Kozikowski AP, Ma A, Papadopoulos V, Puia G, *et al.* 2-Aryl-3-indoleacetamides (FGIN-1): a new class of potent and specific ligands for the mitochondrial DBI receptor. J Pharmacol Exp Ther. 1992;262:971–8.
11. Le Fur G, Terrier ML, Vaucher N, Imbault F, Flamier A, Uzan A, *et al.* Peripheral benzodiazepine binding sites: effect of PK11195, 1-(2-chlorophenyl)-*n*-(1-methylpropyl)-3-isoquinolinecarboxamide I. In vitro studies. Life Sci. 1983;32:1839–47.
12. Marangos PL, Pate J, Boulenger JP, Clark-Rosenberg R. Characterization of peripheral-type benzodiazepine binding sites in brain using [^{3}H]Ro 5–4864. Mol Pharmacol. 1982;22:26–32.
13. Chauveau F, Boutin H, Van Camp N, Dollé F, Tavitian B. Nuclear imaging of neuroinflammation: a comprehensive review of [11C]PK11195 challengers. Eur J Nucl Med Mol Imag. 2008;35:2304–19.
14. Boutin H, Chauveau F, Thominiaux C, Kuhnast B, Grégoire MC, Jan S, *et al.* In vivo imaging of brain lesions with [(11)C] CLINME, a new PET radioligand of peripheral benzodiazepine receptors. Glia. 2007;55:1459–68.
15. Trapani G, Franco M, Latrofa A, Ricciardi L, Carotti A, Serra M, *et al.* Novel 2-phenylimidazo[1,2-*a*]pyridine derivatives as potent and selective ligands for peripheral benzodiazepine receptors. synthesis, binding affinity, and in vivo studies. J Med Chem. 1999;42:3934–41.
16. Trapani G, Laquintana V, Denora N, Trapani A, Lopedota A, Latrofa A, *et al.* Structure-activity relationships and effects on neuroactive steroids in a series of 2-phenylimidazo-[1,2-*a*] pyridineacetamide peripheral benzodiazepine receptors ligands. J Med Chem. 2005;48:292–305.
17. Sekimata K, Hatano K, Ogawa M, Abe J, Magata Y, Biggio G, *et al.* Radiosynthesis and in vivo evaluation of N-[^{11}C]methylated imidazopyridineacetamides as PET tracers for peripheral benzodiazepine receptors. Nucl Med Biol. 2008;35:327–34.
18. Denora N, Laquintana V, Pisu MG, Dore R, Murru L, Latrofa A, *et al.* 2-Phenyl-imidazo[1,2-*a*]pyridine compounds containing hydrophilic groups as potent and selective ligands for peripheral benzodiazepine receptors: synthesis, binding affinity and electrophysiological studies. J Med Chem. 2008;51:6876–88.
19. Kozikowski AP, Kotoula M, Ma D, Boujrad N, Tuckmantel W, Papadopoulos V. Synthesis and biology of a 7-nitro-2,1,3-benzoxadiazol-4-yl derivative of 2-phenylindole-3-acetamide: a fluorescent probe for the peripheral-type benzodiazepine receptor. J Med Chem. 1997;40:2435–9.
20. Manning HC, Goebel T, Thompson RC, Price RR, Lee H, Bornhop DJ. Targeted molecular imaging agents for cellular-scale bimodal imaging. Bioconjugate Chem. 2004;15:1488–95.
21. Manning HC, Smith SM, Sexton M, Haviland S, Bai M, Cederquist K, *et al.* A peripheral benzodiazepine receptor targeted agent for in vitro imaging and screening. Bioconjugate Chem. 2006;17:735–40.
22. Bai M, Rone MB, Papadopoulos V, Bornhop DJ. A novel functional translocator protein ligand for cancer imaging. Bioconjugate Chem. 2007;18:2018–23.
23. Chen Y, Zheng X, Dobhal MP, Gryshuk A, Morgan J, Dougherty TJ, *et al.* Methyl pyrophorbide-R analogues: potential fluorescent probes for the peripheral-type benzodiazepine receptor. Effect of central metal in photosensitizing efficacy. J Med Chem. 2005;48:3692–5.
24. Taliani S, Da Pozzo E, Bellandi M, Bendinelli S, Pugliesi I, Simorini F, *et al.* Novel irreversible fluorescent probes targeting the 18 kDa translocator protein: synthesis and biological characterization. J Med Chem. 2010;53(10):4085–1093.
25. Samuelson LE, Dukes MJ, Hunt CR, Casey JD, Bornhop DJ. TSPO targeted dendrimer imaging agent: synthesis, characterization and cellular internalization. Bioconjugate Chem. 2009;20 (11):2082–9.
26. Laquintana V, Denora N, Lopedota A, Suzuki H, Sawada M, Serra M, *et al. N*-Benzyl-2-(6,8-dichloro-2-(4-chlorophenyl)imidazo[1,2-*a*] pyridin-3-yl)-*N*-(6- (7-nitrobenzo[*c*][1,2,5]oxadiazol-4-ylamino) hexyl)acetamide as a new fluorescent probe for peripheral benzodiazepine receptor and microglial cell visualization. Bioconjugate Chem. 2007;18:1397–407.
27. Clark DE. Rapid calculation of polar molecular surface area and its application to the prediction of transport phenomena. 2. Prediction of blood-brain barrier penetration. J Pharm Sci. 1999;88:815–21.
28. Ertl P, Rohde B, Selzer P. Fast calculation of molecular polar surface area as a sum of fragment-based contributions and its application to the prediction of drug transport properties. J Med Chem. 2000;43:3714–7.